ELSEVIER

PII: S0032-3861(97)00127-4

Polymer Vol. 38 No. 23, pp. 5761–5768, 1997

0032-3861/97/$17.00+0.00

Sorption and longitudinal swelling kinetic behaviour in the system cellulose acetate–methanol

M. Sanopoulou* and J. H. Petropoulos
Physical Chemistry Institute, Demokritos National Research Centre, GR-15310 Aghia Paraskevi, Athens, Greece
(Received 5 August 1996; revised 6 December 1996)

The kinetics of methanol vapour sorption and concurrent longitudinal swelling of cellulose acetate membranes has been studied and interpreted in terms of 'viscous' swelling and differential swelling stress effects, on the basis of previous modelling work. The close parallelism of the kinetic behaviour observed here and in a previous study of the cellulose acetate–acetone system, shows that both sorption and longitudinal swelling kinetics can be understood in terms of the viscoelastic response of the plasticized polymer to an applied osmotic stress, without regard to the nature of the penetrant causing the osmotic stress and plasticization. It has also been shown that, from the first stage of two-stage absorption curves, diffusion coefficient values can be derived agreeing with those evaluated by Takizawa *et al.* from steady state permeation and equilibrium sorption data. © 1997 Elsevier Science Ltd.

(Keywords: non-Fickian sorption; swelling kinetics; cellulose acetate)

INTRODUCTION

In previous papers[1,2], we reported the results of a detailed investigation of various types of deviation from normal Fickian kinetics, which may be observed when a micromolecular vapour is sorbed by a cellulosic polymer. The system cellulose acetate (CA) film–acetone was chosen for study and the experimental work was designed to provide appropriate data for (1) comparison with the earlier work of Bagley and Long[3] and Park[4] (particularly in view of certain significant differences between the results reported by these workers), and (2) more precise identification of the physical origin of the aforementioned non-Fickian anomalies by systematic application of suitable diagnostics derived from earlier modelling work[5–8].

With regard to (1), we concluded that CA films of similar composition but prepared and pretreated in different ways by different workers will still yield consistent results, provided that the said results are analysed in a consistent manner. In particular, Bagley and Long[3] and Park[4] used different methods to extract diffusion coefficient values from their 'two-stage sorption' data (see further discussion below). Application of both methods of analysis to our data reproduced the differences which characterize the results of these authors; and showed that neither set of results could be considered to be fully satisfactory. Further investigation of this point is, therefore, needed. This constitutes one of the main objectives of the present paper.

As far as (2) is concerned, two distinct causes of deviation from Fickian sorption kinetics in glassy polymer films have traditionally been considered, namely[9–11]:

(a) 'delayed (viscous) volume swelling' of the polymer, in response to the osmotic (swelling) stress induced by the penetrant (equivalent to creep induced by a mechanical stress); this results from the fact that relaxation of the polymer molecules to their final equilibrium configurations in the swollen state is a relatively slow process;
(b) 'longitudinal differential swelling stresses (LDSS)', i.e. stresses *along* the plane of the film, induced by the concentration gradients which develop *across* the film during the sorption process (equivalent to the 'thermal stresses' induced by temperature gradients).

On the basis of the sorption and parallel longitudinal swelling kinetic data reported in refs 1 and 2, we were able to elucidate, to a greater extent than had previously proved possible, the role of effects (a) and (b) in determining various aspects of the non-Fickian sorption of a strongly interacting penetrant. It is of considerable interest to compare this case with that of a weakly interacting penetrant. Methanol was chosen for this purpose, with an eye also to our objective under (1); in view of the availability of diffusion coefficient values determined by permeation measurements[12], for comparison with those extracted from two-stage sorption curves. Study of the CA–methanol system is also of interest for practical purposes, in view of the utility of CA membranes for the pervaporative separation of alcohol–water mixtures.

* To whom correspondence should be addressed

THEORY

To treat non-Fickian kinetic behaviour properly, the diffusion equation should, in general, be formulated using the gradient of the chemical potential μ of sorbed penetrant as the driving force of diffusion. For a typical sorption (absorption or desorption) experiment, we have[13]

$$\frac{\partial C}{\partial t} = \frac{\partial}{\partial x}\left(D_T C \frac{\partial \mu}{\partial x}\right) \equiv \frac{\partial}{\partial x}\left(D_T S \frac{\partial a}{\partial x}\right) \qquad (1)$$

where C is the concentration of sorbed penetrant (on a polymer-fixed frame of reference), at position x across the film ($0 \leq x \leq l$, where l is the thickness of the film) and t is time; a is the corresponding activity of the sorbed penetrant, given by $\mu = \mu^0 + RT \ln a$ (which is here equated to the corresponding relative vapour pressure p/p_{sat}); D_T is the thermodynamic diffusion coefficient; and $S = C/a$ is the solubility coefficient, which characterizes the sorption capacity (swellability) of the polymer at the activity and state of relaxation which has been attained at a given x and t. For the systems of interest here, it is not important to make the distinction between D_T and the Fick diffusion coefficient D in common use. Note that $S^0 < S < S^\infty$ ($S^\infty < S < S^0$) in an absorption (desorption) experiment, where S^0 and S^∞ provide a measure of the sorption capacity of the polymer (at any given a) in the unrelaxed and fully relaxed states respectively. The relevant boundary conditions are

$$a(x = 0, l; t) = a_0 = \text{const.};$$
$$a(0 < x < l; t = 0) = a_1 = \text{const.} \qquad (2)$$

where $a_0 > a_1$ and $a_0 < a_1$ for absorption and desorption respectively.

Effect of delayed volume swelling

To model delayed volume swelling in a simple manner, equation (1) is supplemented with[5]

$$\frac{\partial C}{\partial t} = \frac{\partial C^0}{\partial a}\frac{\partial a}{\partial t}\beta(C^\infty - C) \qquad (3)$$

or some analogous expression in other variants of this modelling approach[14–18]. Equation (3) states that the observed increment in swelling at given x and t over a time interval δt, due to influx (in absorption) or outflux (in desorption) of the diffusing penetrant, appears in part as (i) instantaneous (elastic) swelling accompanied by a change in activity, as prescribed by the sorption isotherm of the unrelaxed polymer $C^0 = S^0 a$; and in part as (ii) delayed (viscous) swelling at constant activity, represented as a pseudofirst-order approach to the final sorption equilibrium, defined by $C^\infty = S^\infty a$, at a rate governed by a relaxation frequency (reciprocal relaxation time) β.

Model calculations based on this 'time-dependent solubility or swellability' (TDS) approach have shown[5,14] that the critical parameter governing the observed kinetic behaviour is the rate of relaxation relative to that of diffusion represented by[9] $l^2\beta/D_T$ (often referred to as the Deborah number)[19]. Values of $l^2\beta/D_T \to 0$ or ∞ lead to Fickian kinetics (corresponding to simple diffusion in the unrelaxed or fully relaxed polymer respectively), characterized by Q_t vs $t^{1/2}$ sorption curves (where Q_t is the amount of penetrant sorbed per unit surface area of dry film at time t), which are initially linear through the origin and then become convex upward as the final equilibrium ($Q_t \to Q_\infty$) is approached. A rate of relaxation commensurate with that of diffusion ($l^2\beta/D_T \sim 1$) leads to S-shaped absorption Q_t vs $t^{1/2}$ curves. The corresponding desorption curves are typically found to be convex upward and to cross the absorption ones[9] (but S-shaped desorption curves are possible when D is practically independent of C)[1]. The presence of the viscous relaxation process is confirmed by the fact that, unlike the simple diffusion process, it does not scale with l^2; with the result that plots of Q_t/Q_∞ vs. $t^{1/2}/l$ for films of different thickness do not coincide.

When the relaxation process is sufficiently slow ($l^2\beta/D_T \ll 1$), two-stage absorption curves are obtained[3,4,10,11]. In this case, the first stage represents diffusion of the penetrant in the unrelaxed polymer proceeding to an eventual quasiequilibrium Q_q; while the second stage represents delayed swelling. Thus, if the two stages can be neatly separated, one can study both diffusion and relaxation kinetics directly.

Effect of longitudinal differential swelling stresses

To model the effect of the LDSS [differential swelling stress (DSS) model][6–8] the latter have to be formulated in the same way as thermal stresses, taking due account of the influence of local penetrant concentration on the local mechanical properties of the film. The balance between the tensile and compressive stresses, which develop in the less highly and more highly swollen regions of the film respectively, determines the observed extent of longitudinal swelling of the film ΔL_t.

The extent to which ΔL_t correlates with Q_t will depend on the softening or plasticizing effect of the penetrant on the polymer, manifested as an inverse dependence of the elastic modulus E_s (elastic medium), and a direct dependence of the stress relaxation frequency β_s (viscoelastic medium), on penetrant concentration. In particular, absence of significant deviation from a linear $\Delta L_t/\Delta L_\infty$ vs. Q_t/Q_∞ plot [implying perfect correlation between sorption (S) and longitudinal swelling (LS) kinetics] indicates either (i) no buildup of appreciable LDSS (small concentration gradients) throughout the sorption experiment or (ii) no appreciable variation of E_s and/or β_s over the concentration range covered by the sorption experiment. Model calculations[6–8] indicate that the presence of significant plasticization or softening effects is manifested by negative deviation from the aforesaid linear S–LS correlation in the absorption–dilation mode. A deviation of similar magnitude, but on the positive side of the linear S–LS correlation, is predicted in the desorption–contraction mode, within the bounds of linear elastic or viscoelastic behaviour (i.e. of E_s and β_s independent of the magnitude of the LDSS). In the region of non-linear elastic or viscoelastic behaviour, however, the said deviation tends to become small and negative. These results may be used as diagnostics for the purpose of elucidating the viscoelastic behaviour of the polymer–penetrant system, as illustrated by previous applications to the Nylon 6–water[8] and CA–acetone[2] systems.

Evaluation of the effect of the LDSS on sorption kinetics is based[7] on the tendency of a compressive (tensile) stress to raise (lower) the chemical potential of sorbed penetrant at given C and hence lower (raise) S. Analogous considerations of the effect of stress on free

volume indicate that D_T will tend to be similarly affected by the LDSS. Model calculations[6,7] show that both these effects produce similar deviations from Fickian sorption kinetics. In particular, the DSS model can, like the TDS one, account for S-shaped absorption, associated with convex desorption, Q_t vs. $t^{1/2}$ kinetic curves which cross one another. However, the DSS model goes further and distinguishes between the possibilities that the relevant Q_t/Q_∞ vs. $t^{1/2}/l$ plots for films of different thickness may be coincident or not. The latter possibility arises, as in the TDS model, in the presence of a viscous stress relaxation mechanism (governed by a stress relaxation frequency β_s commensurate with D_T/l^2). The former possibility, which cannot be accounted for by the TDS model, arises if the LDSS relax merely as a result of the decay of the concentration gradients, as diffusion equilibrium is approached. This criterion has enabled us to pinpoint LDSS effects as the cause of non Fickian sorption of acetone by dry CA film up to moderate concentrations[1].

Other kinetic features which can be considered diagnostic for LDSS effects include the observation of higher Q_t values during absorption at small t in thinner membranes[1,9] and concave upward portions of absorption curves plotted on a t scale[1,6,7] ('Super Case II diffusion'). Conversely, the decay of the concentration gradients, and hence of the LDSS, during the first stage of two-stage sorption curves means that the second stage thereof is the manifestation of a TDS effect[1,5].

EXPERIMENTAL

CA powder of 39.8% acetyl content was supplied by Eastman Chemicals (code name E398-30) with the following specifications: melting range 230–250°C; viscosity, measured according to ASTM D-871 (Formula A) and D-1343, 114 poise (30 s). Methanol was of analytical reagent grade.

Films were prepared by casting a 20% solution of the polymer in acetone, on a clean glass surface (instead of a mercury surface as in refs 1 and 2). This was done in order to follow the film preparation procedure of Takizawa *et al.*[12] (bearing in mind the fact that D for glass-cast films may differ substantially from that for mercury-cast films, due to the more intense in-plane macromolecular orientation in the former films). The solution was spread with a knife blade moving on rails and loosely covered for subsequent slow evaporation in an atmosphere partially saturated with acetone vapour. Solvent evaporation was completed in the open atmosphere and then *in vacuo*. In what follows each membrane is designated by a number indicating its thickness in μm.

Parallel sorption and longitudinal swelling equilibrium and kinetic measurements were performed at 25°C on strips cut from the same film. A calibrated quartz spring or a Cahn Electrobalance was used for the former measurements. The latter measurements were performed by means of suitable inductive transducers (Schaevitz, type 0300HR) or a cathetometer. Further details concerning the apparatus and procedures used can be found in refs 1 and 2. The films were first subjected to an annealing treatment in the sorption apparatus by absorption runs over successive small concentration intervals up to the maximum concentration subsequently reached in our experiments. Desorption to $C = 0$ was then effected through the same number of concentration decrements.

RESULTS AND DISCUSSION

Equilibrium sorption and longitudinal swelling

As shown in *Figure 1*, the sorption isotherm was found to exhibit absorption–desorption hysteresis to an extent similar to that previously noted for CA–acetone[1]. Sufficient absorption data have been included in *Figure 1* to show that there was good agreement between the results obtained in different series of sorption runs on the same membrane (series A and B on M135, see below) and on membranes of different thickness, as well as between our data and those of Takizawa *et al.*[12] up to a relative vapour pressure $p/p_{sat} \sim 0.8$. The sorption isotherm duly exhibits the initial convex-upward curvature which characterizes glassy polymer–micromolecular penetrant systems, commonly associated with adsorption in preexisting voids in the polymer matrix (in the present case, the tendency of hydrogen bond formation with polymer hydroxyl groups may also play a significant role in this respect).

The degree of longitudinal swelling (LS) expressed as the fractional elongation $L(C)/L(0) - 1$ (where L is the measured length of the film), varied approximately linearly with penetrant concentration C, and the results obtained were very close to those found for acetone, when C is expressed in g per unit volume of dry polymer, as illustrated in *Figure 2*. This similarity stems from the closeness of the liquid density of these penetrants; which means that equal values of C represent very nearly equal volumes of sorbent liquid penetrant and hence very similar degrees of volume swelling, if volume additivity of mixing is not grossly violated. Note that the acetone data reported in *Figure 2* (line c) refer to glass-cast membranes, which yield a considerably lower degree of LS than that found in mercury-cast ones (illustrated by line d in *Figure 2*), due to the much more pronounced in-plane preferred macromolecular orientation of the former membranes (the discrepancy

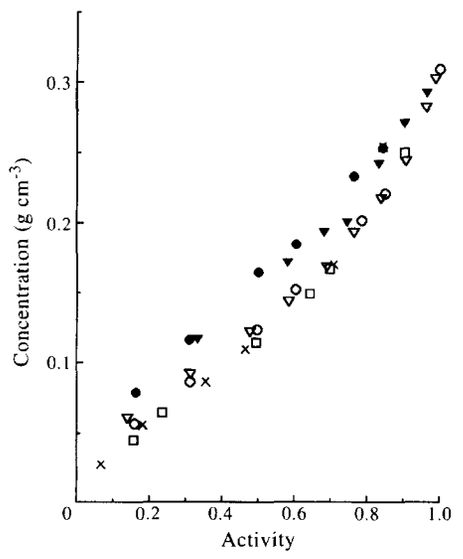

Figure 1 Sorption isotherm for the system cellulose acetate–methanol at 25°C. Absorption: M135, series A (○); M135, series B (▽); M65 (□). Desorption: M135, series A (●); M135; series B (▼). Corresponding absorption data of Takizawa *et al.*[12]: (×)

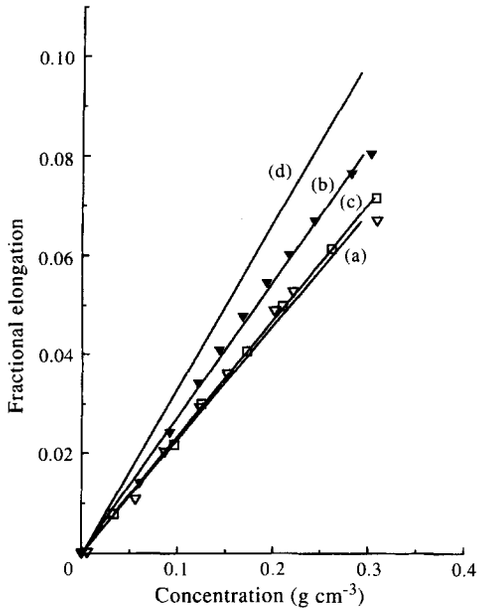

Figure 2 Concentration dependence of the fractional elongation $L(C)/L(0) - 1$ of glass-cast CA membranes, based on equilibrium sorption and elongation data obtained from series of successive absorption runs of (i) methanol in M135: series A (line a, ▽); series B (line b, ▼) or (ii) acetone in M243 (line c, □). Line d refers to absorption of acetone in a mercury-cast membrane M59 (line A of Figure 9 of ref. 2)

between line d and the remaining ones of *Figure 2* may serve as an indication of the degree of swelling anisotropy which characterizes the relevant glass-cast membranes). *Figure 2* (cf. lines a and b) also illustrate the point that taking a glass-cast membrane through a complete absorption–desorption cycle ($p = 0 \rightarrow p_{sat} \rightarrow 0$) was accompanied by significant slow irreversible macromolecular reorientation; which resulted in substantial reduction of the aforesaid swelling anisotropy (cf. lines a, b), without significant change in volume swelling (as indicated by the unchanged equilibrium sorption in *Figure 1*). This results in permanent reduction of the dry film length $L(0)$ and suggests that the use of an inappropriate value of $L(0)$ may be the main reason why the uppermost points belonging to line a (and line b to a lesser extent) tend to fall significantly below their expected positions. On the other hand, similar discrepancies at the low concentration end of the said lines are consistent with filling of the excess free volume of the polymer. The fact that such an effect is much less evident in the case of acetone (line c), is in keeping with our previous inference from a study of liquid penetration profiles that methanol can (presumably because of its smaller molecular size) fill the excess free volume of CA more efficiently than acetone[20].

Sorption and longitudinal swelling kinetics

Two series (designated as A and B) of successive absorption kinetic runs, in which the final activity $a_{0,n}$ (corresponding concentration $C_{0,n} = S^{\infty} a_{0,n}$) of the nth run served as the initial activity $a_{1,n+1}$ (corresponding concentration, $C_{1,n+1} = S^{\infty} a_{1,n+1}$) of the $(n+1)$th run (i.e. $a_{0,n} \equiv a_{1,n+1}$; $C_{0,n} \equiv C_{1,n+1}$), were performed on membrane M135. In series A, the concentration intervals $\Delta C_n = C_{0,n} - C_{0,n-1}$ were kept as small as was consistent with reasonably accurate measurement of penetrant uptake and elongation of the membrane. In series B,

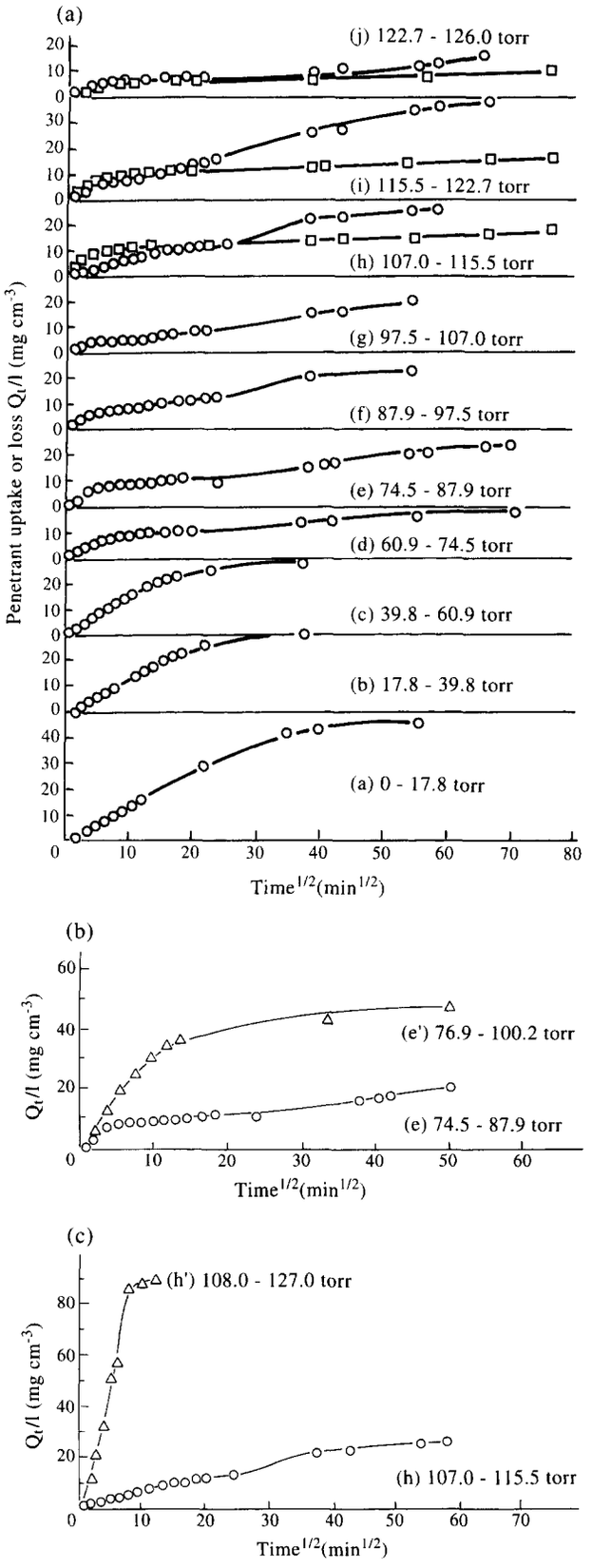

Figure 3 (a) Series A of successive absorption (○) and desorption (□) kinetic runs of methanol in M135. Desorption runs were performed in sequence after all absorption runs were completed. (b) Comparison of absorption run (*e*) of series A (○) with a corresponding absorption run (*e'*) of series B (△) on M135. Run (*e'*) has approximately the same C_1 ($\sim 0.14\,g\,cm^{-3}$) with run (*e*) but covers a concentration interval ΔC ($\sim 0.05\,g\,cm^{-3}$) approximately equal to the sum of ΔC's of runs (*e*) and (*f*). (c) Comparison of absorption run (*h*) of series A (○) with a corresponding absorption run (*h'*) of series B (△) on M135. Run (*h'*) has approximately the same C_1 ($\sim 0.22\,g\,cm^{-3}$) with run (*h*) but covers a concentration interval ΔC ($\sim 0.09\,g\,cm^{-3}$) approximately equal to the sum of ΔC's of runs (*h*), (*i*) and (*j*)

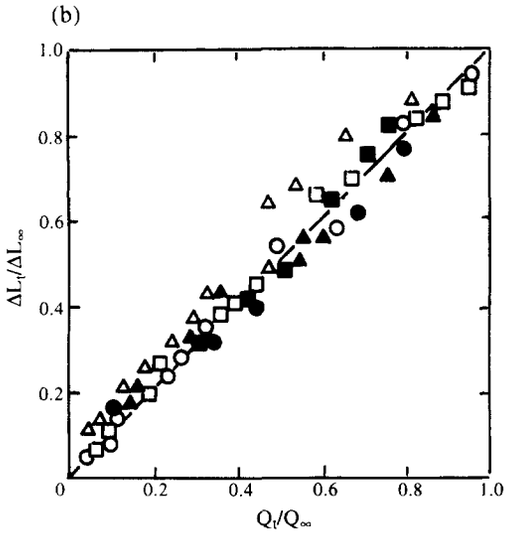

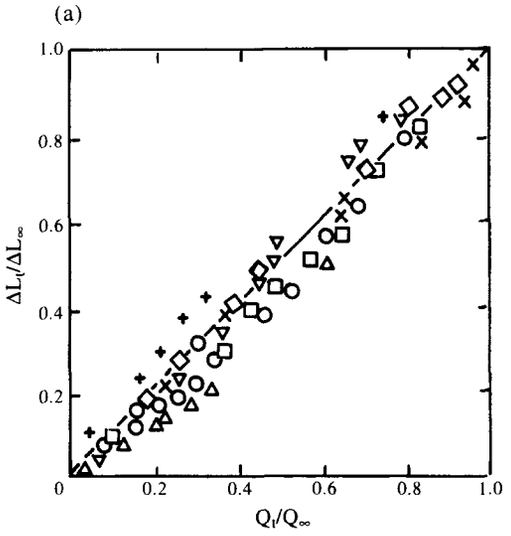

Figure 4 S–LS kinetic correlations for the successive sorption runs on M135 presented in *Figure 3a*. (a) Absorption runs: $p_0 = 17.8$ (○); 39.8 (△); 60.9 (□); 74.5 (▽); 87.9 (×); 97.5 (◇); 107.0 (+) torr [corresponding C_0: 0.060 (○); 0.091 (△); 0.122 (□); 0.143 (▽); 0.168 (×); 0.193 (◇); 0.217 (+) g cm^{-3}]. (b) Absorption runs: $p_0 = 115.5$ (△); 122.7 (□); 126.0 (○) torr [corresponding C_0: 0.244 (△); 0.282 (□); 0.302 (○) g cm^{-3}]. Desorption runs: $p_0 = 123.0$ (▲); 115.0 (■); 106.1 (●) torr [corresponding C_0: 0.292 (▲); 0.271 (■); 0.242 (●) g cm^{-3}]

considerably larger ΔC_n were used. The absorption runs in series A were followed by three desorption runs, and the corresponding penetrant uptake or loss data are shown in *Figure 3a*. Comparison of selected absorption runs of series A with corresponding selected runs of series B are presented in *Figures 3b* and *c*. The LS kinetic data corresponding to the sorption data of *Figure 3a* are presented, in the form of S–LS kinetic correlations, in *Figure 4*.

A series of 'integral' absorption (coupled with corresponding desorption) runs was also performed on M135, in which $a_1 = 0$ ($C_1 \approx 0$) in all runs, while a_0 (and hence $C_0 \approx \Delta C$) was varied from one run to the next. The results obtained are presented in *Figure 5*. For the

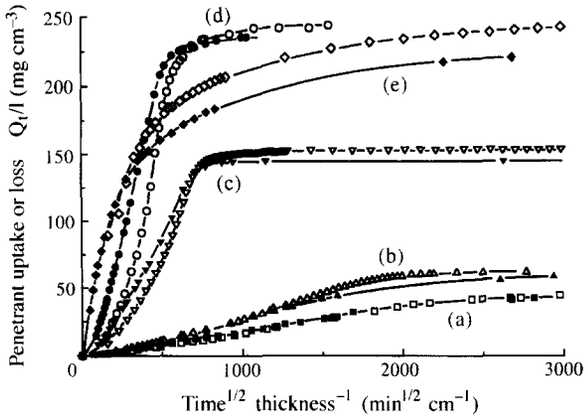

Figure 5 Integral sorption runs on membranes M65 (open points) and M135 (filled points). Absorption: $p_1 = 0$ ($C_1 \sim 0$); $p_0 = 20$ (curves a, □, ■); 30 (curves b, △, ▲); 82 (curves c, ▽, ▼); 115 (curves d, ○, ●) [corresponding $\Delta C = 47$ (curves a); 64 (curves b); 150 (curves c); 240 (curves d) mg cm^{-3}]. Desorption: $p_0 = 0$ ($C_0 \sim 0$); $p_1 = 115$ torr, $\Delta C \sim 230$ mg cm^{-3} (curves e, ◇, ◆)

sake of clarity, the desorption data are given only in one case. The corresponding S–LS correlations are shown in *Figure 6*. The effect of film thickness was investigated by repeating the aforesaid measurements on a thinner membrane (M65). The results obtained are included in *Figures 5* and *6*.

The above results present a picture of sorption and longitudinal swelling kinetic behaviour which is closely similar, in all main aspects, to that previously established in studies of CA–acetone[1–4].

Thus, *Figure 3a* shows the familiar progressive change of the absorption curves (expressed in the form Q_t/l vs. $t^{1/2}$ plots) in series A from S-shaped at the low, to two-stage at the high, concentration end; while *Figure 5* shows that the rate of sorption increases, and the aforesaid S shape is intensified, with rising ΔC. *Figure 5* further demonstrates that plots of Q_t/l for approximately the same value of ΔC (which is approximately equivalent to Q_t/Q_∞) vs. $t^{1/2}/l$ for M135 and M65 are coincident at lower ΔC (curves a and b), pointing to (elastic) LDSS as the only possible cause of the S shape, as previously indicated (see theoretical section and ref. 1). This interpretation is also consistent with the observation of higher penetrant uptake per unit area Q_t at small times by M65 than by M135 (see *Figure 7* and the theoretical section) and with the tendency of the S shape to disappear at low ΔC (bearing in mind that low ΔC implies weak LDSS). Evidence, in the form of discrepancy between the aforementioned M135 and M65 Q_t/l vs. $t^{1/2}/l$ plots, of the presence of a viscous relaxation process appears only at higher ΔC values (curves c and d of *Figure 5*). According to both the TDS and the DSS model, a rise in the relative relaxation frequency ($l^2\beta/D$ or $l^2\beta_s/D$ respectively) should enhance (reduce) the rate of absorption (desorption)[5–7]. In line with this prediction, the high ΔC absorption (desorption) plots of *Figure 5* for the thicker membrane lie above (below) the corresponding ones for the thinner one. In the case of the desorption plots, the discrepancy is clearly visible in the later part of the curves (because the initial steep part extends over a time interval which, even in the case of the thick membrane, is too short for substantial relaxation to occur).

Comparison of *Figure 5* with the corresponding data

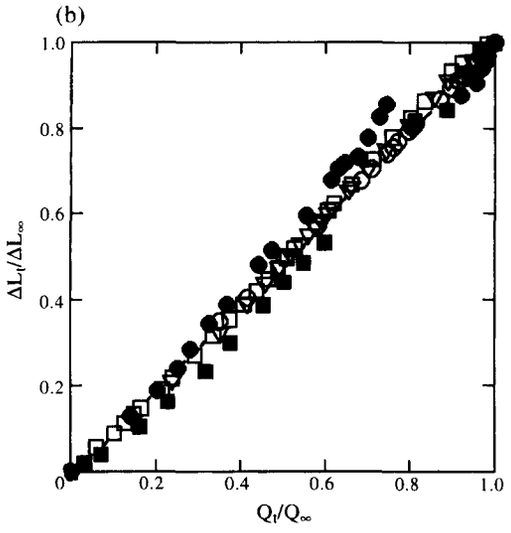

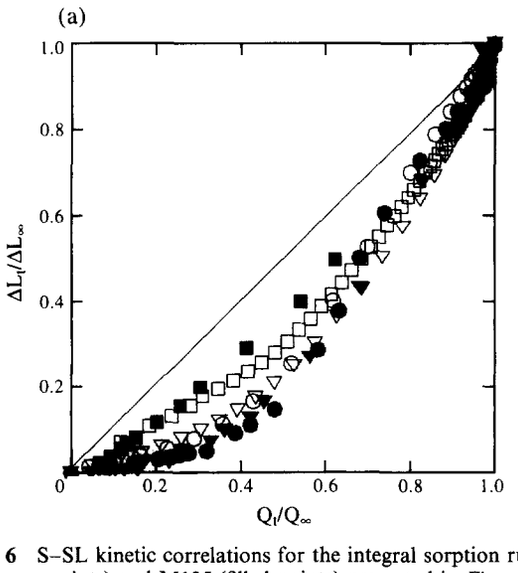

Figure 6 S–SL kinetic correlations for the integral sorption runs on M65 (open points) and M135 (filled points) presented in *Figure 5*. (a) Absorption (same symbols and notation as in *Figure 5*): $p_1 = 0$; $p_0 = 20$ (□, ■); 82 (▽, ▼); 115 (○, ●) torr. (b) Desorption [same symbols and notation as in (a)]: $p_0 = 0$; $p_1 = 20$ (□, ■); 82 (▽); 115 (○, ●)

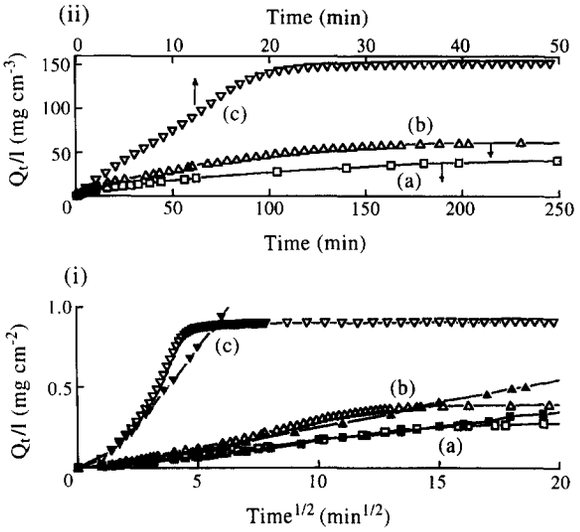

Figure 7 Selected integral absorption runs from *Figure 5* plotted in (i) Q_t vs. $t^{1/2}$; (ii) Q_t/l vs. t. Symbols and notation as in *Figure 5*

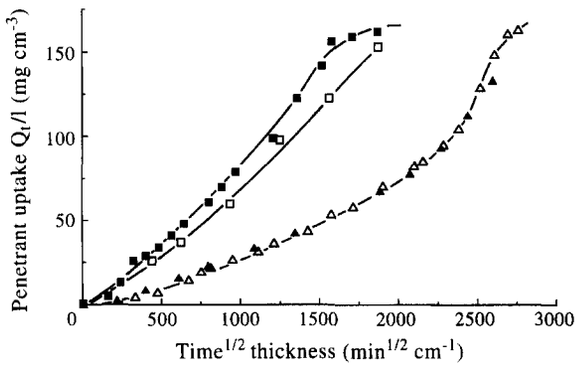

Figure 8 Integral absorption runs at 30°C, with $p_1 = 0$ and $p_0 = 120$ torr, of acetone in (i) mercury-cast membranes M42 (△) and M112 (▲) [lower set of curves in Figure 6a of ref. 1] and (ii) glass-cast membranes M32 (□) and M124 (■)

of ref. 1 (cf. *Figure 6* therein) shows that the said viscous stress—relaxation mechanism appears at lower ΔC here. For example, the 0–82 torr experiment (curves c in *Figure 5* here) and the 0–120 torr experiment in Figure 6 of ref. 1 correspond to approximately the same ΔC (150 and 170 mg cm^{-3} respectively) but the latter (in contrast to the former) shows no evidence of viscous relaxation. To establish whether this difference in kinetic behaviour is attributable chiefly to the membrane preparation technique (casting on glass or on mercury) or to the nature of the penetrant (methanol vs. acetone) the 0–120 torr acetone absorption runs were repeated using glass-cast membranes M32 and M124. The results, given in *Figure 8*, show that the structural differences in the membrane induced by the casting technique can account for the aforementioned difference in kinetic behaviour.

The S–LS kinetic correlation pattern presented in *Figure 6* resembles closely that shown in ref. 2. As noted therein, the substantial observed deviations of the absorption–dilation plots from linearity (*Figure 6a*) constitute direct evidence of (a) the existence of LDSS of significant magnitude and (b) the presence of plasticization effects; while the small corresponding deviations exhibited by the corresponding desorption–contraction plots (*Figure 6b*) are consistent with non-linear viscoelastic behaviour. Comparison of the absorption–dilation plot for the lowest ΔC in *Figure 6a* (ΔC = 47 mg cm^{-3}) with that of a comparable acetone run (ΔC = 51 mg cm^{-3}; see Figure 11 of ref. 2) shows that the deviation from linearity is more pronounced in the latter case. This suggests that the LDSS generated in the present system are weaker and is in line with (a) the less extensive LS of glass-cast membranes, and (b) the tendency of methanol to swell the polymer less strongly than acetone at low C, as noted above.

The two-stage sorption behaviour which characterizes the high concentration end of series A follows closely the pattern established in ref. 1. In particular, the rate of the second stage is insensitive to changes in C [see curves d–j in *Figure 3a*], but increases markedly with rising ΔC [with the result that the two stages tend to merge to a greater or lesser extent, as illustrated by curves (*e*), (*e'*) and (*h*), (*h'*) in *Figures 3b* and *c* respectively]; while the

S–LS correlation does not deviate materially from linearity (see *Figure 4*) in both absorption–dilation and desorption–contraction modes (in keeping with the weakness or absence of LDSS or of the relevant softening effects[2]). The first and second stages of these curves were analysed separately to obtain estimates of the diffusion coefficient and the relaxation frequency respectively, as described below.

Evaluation of the diffusion coefficient

Values of the diffusion coefficient were calculated from the first stage of two-stage absorption curves, using the short time approximation

$$\frac{Q_t}{Q_q} = 4\left(\frac{Dt}{\pi l^2}\right)^{1/2} \tag{4}$$

The dry film thickness was used for l (polymer–fixed frame of reference) and the amount of penetrant corresponding to the quasi-equilibrium which marks the end of the first stage Q_q was estimated either (a) by simple extrapolation of the flat initial portion of the second stage to $t = 0$ (method of Bagley and Long)[3] or (b) by iterative readjustment of the aforementioned estimate of Q_q, until equation (4) and the corresponding long-time approximation

$$\frac{Q_t}{Q_\infty} = 1 - \frac{8}{\pi^2}\exp\left(-\frac{D\pi^2 t}{l^2}\right)$$

gave the same result for D, on the assumption that $D \cong$ const. over the relevant concentration interval $C_q - C_1$ (method of Park)[4]. The short-time Q_t/l vs. $t^{1/2}$ plots obtained here were found to conform to linearity more closely than was the case in ref. 1 (where a distinct tendency of these plots to be S-shaped was noted). This is probably due, at least in part, to the generally narrower concentration intervals used here (which also favour closer conformity to the assumption of $D \cong$ const. mentioned above). In agreement with our findings in the case of CA–acetone[1], the method of Bagley and Long tended to yield higher D values than the method of Park. The results obtained by both methods, in the concentration range where comparison with those of Takizawa *et al.*[12] is possible, are given in *Figure 9*. To effect this comparison, the integral diffusion coefficient $\bar{D}(C_0)$ given by Takizawa *et al.* were converted to the corresponding differential values

$$D(C_0) = C_0 \frac{\mathrm{d}\bar{D}(C_0)}{\mathrm{d}C_0} + \bar{D}(C_0)$$

which are shown in *Figure 9* to agree reasonably well with the results of Park's method.

Evaluation of delayed swelling kinetics

When the second stage of a two-stage sorption curve is well separated from the first stage, it may be assumed to represent pure relaxation (delayed swelling) kinetics. One then has the opportunity to test directly the first-order relaxation kinetic law postulated by the TDS model. The latter is represented by equation (3) with $\partial a/\partial t = 0$ and $\beta =$ const.; the integrated form of which may be written

$$1 - \frac{Q_t}{Q_\infty} = \left(1 - \frac{Q_q}{Q_\infty}\right)\exp(-\beta t) \tag{5}$$

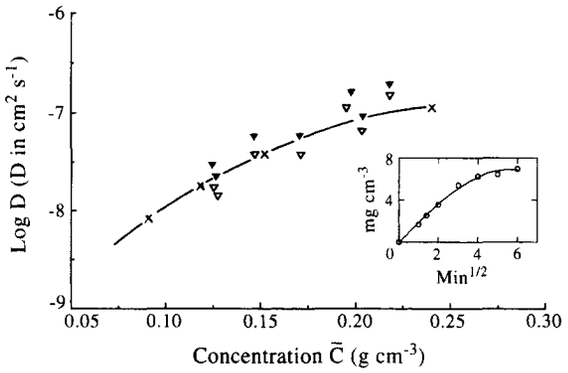

Figure 9 Diffusion coefficients, derived by the method of Park[4] (▽) or of Bagley and Long[3] (▼) from two-stage absorption runs on M135, plotted as a function of the mean concentration $\bar{C} = C_1 + (C_q - C_1)/2$ of penetrant over the applicable concentration range. Diffusion coefficients obtained from permeation and equilibrium sorption measurements by Takizawa *et al.*[12] (line, ×). Inset: Enlarged plot of the first stage of two-stage absorption curve (f) of *Figure 3a*

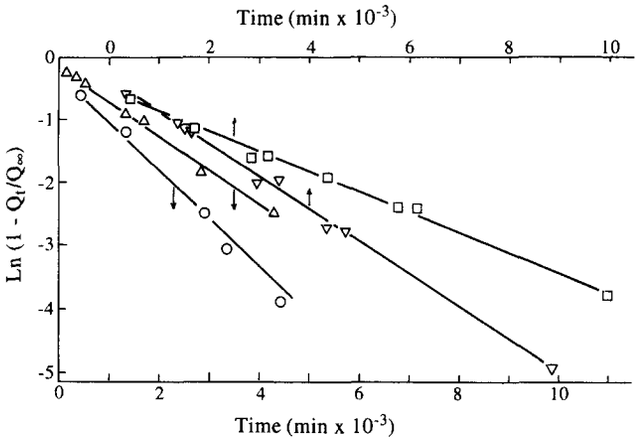

Figure 10 First order plots of the second stage of absorption on M135. C_1: 0.112; (□); 0.143 (▽); 0.201 (△); 0.244 (○) g cm^{-3}; ΔC: 0.0216 (□); 0.0249 (▽); 0.0194 (△); 0.0376 (○) g cm^{-3}; $\beta \times 10^4$: 2.94 (□); 5.13 (▽); 5.43 (△); 8.14 (○) min^{-1}

As illustrated by the plots based on equation (5) in *Figure 10*, conformity of the second-stage data obtained here to first-order kinetics is good; considerably better, in fact, than was previously found for the mercury-cast CA membrane–acetone system studied in ref. 1; probably as a result of better separation of first and second stages achieved here. The β values derived from these plots ($\beta \sim 5 \times 10^{-4}$ min^{-1} for $\Delta C \sim 0.03$ g cm^{-3}) are very similar to those found in ref. 1 and exhibit closely analogous behaviour, as regards both their strong dependence on the magnitude of ΔC and the virtual lack of such dependence on the value of C_1 (as illustrated by the marked acceleration of the second stage in two-stage sorption curves in series B when compared with analogous ones of series A and by the lack of such an effect with increasing C_1 within series A; see *Figures 3b, c* and *a* respectively).

By analogy with viscous creep under a mechanical stress, volume relaxation represented by the second stage may be regarded as occurring under an osmotic stress σ_v; which, according to Newns[21], is given by

$$\sigma_v = \frac{RT}{\bar{V}_A} \ln \frac{a_0}{a_q} \tag{6}$$

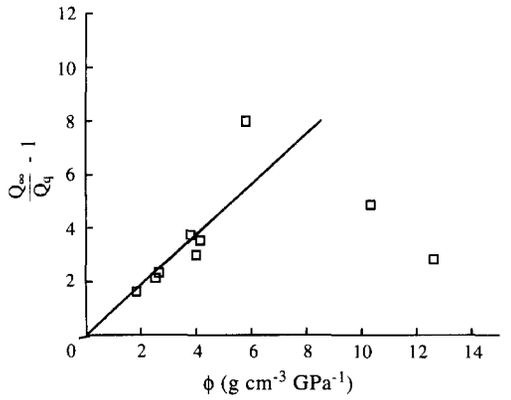

Figure 11 Correlation of the fractional amount sorbed during the first stage of absorption runs of methanol in M135 with activity according to equation (8) compared with the regression line representing the corresponding data for acetone[1]

and can be related to first-stage elastic swelling via a modulus B, namely

$$\sigma_v = B\Delta v_q = BQ_q/l\rho_A \tag{7}$$

In equations (6) and (7), a_q is the activity, which, according to the sorption isotherm, corresponds to C_q; Δv_q is the fractional (elastic) swelling of the polymer caused by the uptake Q_q; $\bar{V}_A$ is the molar volume of the liquid penetrant; and ρ_A is the apparent density of the sorbed penetrant. Newns' treatment predicts that Q_q/Q_∞ should decrease with increasing activity, according to the approximate relation

$$\frac{Q_\infty}{Q_q} \approx 1 + \frac{2\Delta C\bar{V}_A B a_q}{\Delta aRT\rho_A(3 - a_0/a_q)} = 1 + \frac{B}{\rho_A}\phi \tag{8}$$

The results obtained here are presented in *Figure 11* together with the regression line, which represents the corresponding CA–acetone data of ref. 1 and yields $B \approx 0.7$ GPa. The data of methanol appear to follow the trend predicted by equation (8) and to agree reasonably well with the acetone data in the range where the latter were available. The observed deviation at higher abscissa values (i.e. at higher concentrations of sorbed methanol) is similar to that found by Newns in the system cellulose–water[21] and was attributed by him to a significant decrease of B due to plasticization.

CONCLUSION

The conclusions drawn from the present work, in relation to the main objectives stated in the introductory section, may be summarized as follows: (1) under conditions of good separation of the first and second stages of two-stage absorption curves, the previously observed discrepancies in the diffusion coefficient values estimated from the first stage by the method of Bagley and Long and the method of Park can be considerably reduced. The latter estimates are in better agreement with those derived by Takizawa *et al.* from steady-state permeation and equilibrium sorption data; thus conforming previous tentative conclusions in favour of the Park's method[1].

(2) In spite of the facts that (i) acetone is a solvent for CA, while methanol is a weak swelling agent and (ii) these penetrants tend to interact preferentially with different groups of the polymer (namely acetate and hydroxyl groups respectively); the sorption and longitudinal swelling kinetic behaviour of CA–methanol parallels very closely that of CA–acetone (apart from some minor differences attributable to the ability of methanol to fill excess free volume more efficiently than acetone, in the low concentration region). This close similarity extends to the magnitude of the relaxation frequency β and the osmotic elastic modulus B and is consistent with a general picture of sorption and LS kinetics being determined by the viscoelastic response of the plasticized polymer to an applied osmotic stress, without regard to the nature of the penetrant that is causing the osmotic stress and plasticization.

REFERENCES

1. Sanopoulou, M., Roussis, P. P. and Petropoulos, J. H., *J. Polym. Sci.: Part B: Polym. Phys.*, 1995, **33**, 993.
2. Sanopoulou, M., Roussis, P. P. and Petropoulos, J. H., *J. Polym. Sci.: Part B: Polym. Phys.*, 1995, **33**, 2125.
3. Bagley, E. and Long, F. A., *J. Am. Chem. Soc.*, 1955, **77**, 2172.
4. Park, G. S., *Trans. Faraday Soc.*, 1961, **57**, 2314.
5. Petropoulos, J. H., *J. Polym. Sci., Polym. Phys. Ed.*, 1984, **22**, 1885.
6. Petropoulos, J. H. and Roussis, P. P., *J. Membrane Sci.*, 1978, **3**, 343.
7. Petropoulos, J. H., *J. Membrane Sci.*, 1984, **18**, 37.
8. Petropoulos, J. H., *J. Membrane Sci.*, 1984, **17**, 233.
9. Crank, J., *J. Polym. Sci.*, 1953, **11**, 151.
10. Long, F. A. and Richman, D., *J. Am. Chem. Soc.*, 1960, **82**, 513.
11. Fujita, H., *Adv. Polym. Sci.*, 1961, **3**, 1.
12. Takizawa, A., Kinoshita, T., Sasaki, M. and Tsujita, Y., *J. Membrane Sci.*, 1980, **6**, 265.
13. Petropoulos, J. H. and Roussis, P. P., *J. Chem. Phys.*, 1967, **47**, 1491.
14. Durning, C. J., *J. Polym. Sci., Polym. Phys. Ed.*, 1985, **23**, 1831.
15. Durning, C. J. and Tabor, M., *Macromolecules*, 1986, **19**, 2220.
16. Cox, R. W. and Cohen, D. S., *J. Polym. Sci., Polym. Phys. Ed.*, 1989, **27**, 589.
17. Wu, J. C. and Peppas, N. A., *J. Polym. Sci.: Part B: Polym. Phys.*, 1993, **31**, 1503.
18. Kim, M. and Neogi, P., *J. Appl. Polym. Sci.*, 1984, **29**, 731.
19. Vrentas, J. S., Jarzebski, C. M. and Duda, J. L., *AIChE J.*, 1975, **21**, 894.
20. Sanopoulou, M. and Petropoulos, J. H., *J. Polym. Sci., Part B: Polym. Phys.*, 1992, **30**, 971.
21. Newns, A. C., *Trans. Faraday Soc.*, 1956, **52**, 1533.